Inorg. Chem. **2006**, *45*, 688–694

Orbital Angular Momentum Contribution to the Magneto-Optical Behavior of a Binuclear Cobalt(II) Complex

S. M. Ostrovsky,*,† K. Falk,‡ J. Pelikan,‡ D. A. Brown,§ Z. Tomkowicz,|| and W. Haase‡

Institute of Applied Physics, Academy of Sciences of Moldova, Academy str. 5, MD-2028 Chisinau, Moldova, Eduard-Zintl-Institute of Inorganic and Physical Chemistry, Darmstadt University of Technology, Petersenstrasse 20, D-64287 Darmstadt, Germany, Department of Chemistry, University College, Belfield, Dublin 4, Ireland, and Institute of Physics, Jagiellonian University, 30-059 Krakow, Poland

Received August 28, 2005

We report magnetic and magnetic circular dichroism investigations of a binuclear Co(II) compound. The Hamiltonian of the system involves an isotropic exchange interaction dealing with the real spins of cobalt(II) ions, spin–orbit coupling, and a low-symmetry crystal field acting within the $^4T_{1g}$ ground manifold of each cobalt ion. It is shown that spin–orbit coupling between this ground term and the low-lying excited ones can be taken into consideration as an effective *g* factor in the Zeeman part of the Hamiltonian. The value of this *g* factor is estimated for the averaged experimental values of Racah and cubic ligand field parameters for high-spin cobalt(II). The treatment of the Hamiltonian is performed with the use of a irreducible tensor operator technique. The results of the calculation are in good agreement with experimental observations. Both a large effective *g* factor for the ground state and a large temperature-independent part of the magnetic susceptibility arise because of a strong orbital contribution to the magnetic behavior of the Co(II) dimer.

I. Introduction

Metallohydrolases with peptidase or phosphoesterase activity are of considerable interest to bioinorganic chemists because of their essential role in living organisms. Most of the well-studied examples contain a single metal ion that is involved in the enzymatic reaction. However, the number of binuclear metallohydrolases is growing rapidly. The common structural feature of these metallohydrolases is a dinuclear metal active site featuring Zn(II), Ni(II), Co(II), or Mn(II). The possibility that these metalloenzymes can be used in different therapeutic applications has led to growing interest in the characterization and modeling as well as the theoretical descriptions of such compounds.[1−4]

From a theoretical point of view, the most interesting but complicated situation is in the case of the interaction of two Co(II) ions in octahedral surroundings. The $^4T_{1g}$ ground state is orbitally degenerate. This orbital degeneracy leads to highly anisotropic interactions, and the effective exchange Hamiltonian contains not only spin operators but also orbital ones.[5] In general, the isotropic Heisenberg−Dirac−Van Vleck (HDVV) model should be improved by taking into account special forms of orbitally dependent exchange interactions.[6,7] Recently, Tsukerblat et al.[8] presented magnetic investigations of a trinuclear iron−cobalt complex. Following the idea of Lines,[9] these authors neglected orbitally dependent terms of the exchange interaction between Co(II) and Fe(III) ions and took into consideration only the isotropic exchange

* To whom correspondence should be addressed. E-mail: sm_ostrovsky@yahoo.com.
† Academy of Sciences of Moldova.
‡ Darmstadt University of Technology.
§ University College.
|| Jagiellonian University.

(1) Beckett, R. P.; Davidson, A. H.; Drummond, A. H.; Huxley, P.; Whitetaker, M. *Drug Discovery Today* **1996**, *1*, 16.
(2) Wilcox, D. E. *Chem. Rev.* **1996**, *96*, 2435.
(3) Dixon, N. E.; Reddles, P. W.; Gazzola, C.; Blakeley, R. L.; Zerner, B. *Can. J. Biochem.* **1980**, *58*, 1335.
(4) Arnold, M.; Brown, D. A.; Deeg, O.; Errington, W.; Haase, W.; Herlihy, K.; Kemp, T. J.; Nimir, H.; Werner, R. *Inorg. Chem.* **1998**, *37*, 2920.
(5) Levy, P. M. *Phys. Rev.* **1969**, *177*, 509.
(6) Borras-Almenar, J. J.; Clemente-Juan, J. M.; Coronado, E.; Palii, A. V.; Tsukerblat, B. S. *J. Phys. Chem. A* **1998**, *102*, 200.
(7) Borras-Almenar, J. J.; Clemente-Juan, J. M.; Coronado, E.; Palii, A. V.; Tsukerblat, B. S. *J. Chem. Phys.* **2001**, *114*, 1148.
(8) Tsukerblat, B. S.; Palii, A. V.; Mirovitskii, V. Yu.; Ostrovsky, S. M.; Turta, K.; Jovmir, T.; Shova, S.; Bartolome, J.; Evangelisti, M.; Filoti, G. *J. Chem. Phys.* **2001**, *115*, 9528.
(9) Lines, M. E. *J. Chem. Phys.* **1971**, *55*, 2977.

10.1021/ic0514748 CCC: $33.50
Published on Web 12/24/2005

between real spins. The orbital degeneracy of high-spin cobalt was taken into account by the inclusion of the orbital momentum of the $^4T_{1g}$ term and the spin−orbit coupling within this term. The importance of the orbital contribution to the magnetic behavior was demonstrated.

In this Article, we report the magnetic and magnetic circular dichroism investigations of a Co(II) dimeric compound. The approach proposed in ref 8 is modified by taking into consideration the spin−orbit coupling between the $^4T_{1g}$ ground term and the low-lying excited ones. The proposed model is applied to the study of the $[Co_2(\mu\text{-OAc})_3(\text{urea})(\text{tmen})_2][\text{OTf}]$ complex. The obtained results clearly demonstrate a strong orbital contribution to the magnetic properties of the investigated compound.

II. Experimental Section

Magnetic Measurements. The magnetic susceptibility of a polycrystalline sample was recorded using a computer-controlled Faraday-type balance Cahn D-200 in a temperature range of 4.5−300 K at the applied field of 0.5 T. The susceptibility data were corrected for diamagnetic contributions as deduced with the use of Pascal's constant tables.

MCD Measurements. MCD spectra were measured using a JASCO J-810 spectropolarimeter, interfaced with an Oxford instruments cryostat Spectromag SM 4000-9T equipped with a split-coil superconducting magnet. The measurements were performed in the selected temperature range of 3−20 K and the selected wavelength range of 375−625 nm. The sample was mixed with Nujol and placed between two thin quartz plates in a copper sample holder that was screwed to the lower end of the sample probe. The temperature was regulated by adjusting the helium gas flow rate from the main bath through the heat exchanger and by using two pairs of heaters and thermometers mounted at the heat exchanger and at the sample probe located near the sample. The accuracy of the temperature control was better than 0.3 K. The cryostat windows and the sample holder were checked to make sure that they were not giving out MCD signals. Data acquisition was achieved using JASCO spectra manager software. The obtained MCD spectra were corrected by subtracting the small zero-field MCD signal.

III. Model

The crystal structure of the investigated Co(II) dimer is shown in Figure 1. Each cobalt ion is octahedral coordinated, but the site symmetry is lower because of some distortions in the surroundings. One can see that this symmetry is D_{2h} at best. The local z_i axes ($i = 1, 2$) are chosen to be parallel to the O1−O7 direction for Co1 and the O2−O5 direction for Co2. The local x_1 axis is parallel to the bisector of the N1−Co1−N2 angle, whereas the x_2 axis is parallel to the bisector of the N3−Co2−N4 angle. The local y_i axis for each Co ion is perpendicular to the corresponding x_iz_i plane.

All calculations are performed in the molecular coordinate system (XYZ), which is as follows: The Z axis is parallel to the bisector of the angle between the local z_i axes, the X axis lies in the plane of the local z_1z_2 axes, and the Y axis is perpendicular to the XZ plane. The unitary transformation

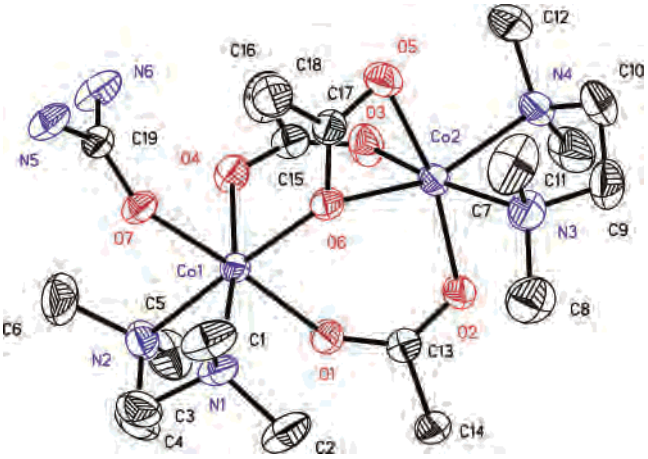

Figure 1. Molecular structure of $[Co_2(\mu\text{-OAc})_3(\text{urea})(\text{tmen})_2][\text{OTf}]$.

from the molecular coordinate system to the local ones is given by $\mathbf{A}(i)$ matrixes

$$\mathbf{A}(i) = \begin{pmatrix} \cos\beta_i\cos\gamma_i & -\cos\beta_i\sin\gamma_i & \sin\beta_i \\ \sin\gamma_i & \cos\gamma_i & 0 \\ -\sin\beta_i\cos\gamma_i & \sin\beta_i\sin\gamma_i & \cos\beta_i \end{pmatrix} \quad (1)$$

where β_i and γ_i are the Euler angles.

The Hamiltonian of the investigated Co dimer can be written as

$$\mathbf{H} = \mathbf{H}_{SO} + \mathbf{H}_{cr} + \mathbf{H}_{ex} + \mathbf{H}_{Ze} \quad (2)$$

The first part in eq 2 represents the spin−orbit coupling. The ground state of Co(II) is orbitally degenerate ($^4T_{1g}$ triplet in a cubic crystal field). Focusing on the $^4T_{1g}$ ground state only (it corresponds to the assumption that the ligand field is strong enough), we can describe Co(II) as an ion with the spin value $S = {}^3/_2$ and the fictitious angular momentum $L = 1$. The spin−orbit interaction within the $^4T_{1g}$ triplet can be written as follows

$$\mathbf{H}^i_{SO} = -\frac{3}{2}\kappa\lambda\mathbf{S}_i\mathbf{L}_i \qquad (i = 1, 2) \quad (3)$$

where κ is the orbital reduction factor and λ is the spin−orbit coupling parameter (-170 cm^{-1}) for a free Co(II) ion. The factor $^{-3}/_2$ appears because the matrix elements of $\mathbf{L}$ within the $^4T_{1g}$ states are exactly the same as the matrix elements of $-3\mathbf{L}/2$ within the p basis. It should also be mentioned that the orbital reduction factor κ takes into account not only the covalence of the cobalt−ligand bonds but also the mixture of both $^4T_{1g}$ states (originating from ^4F and ^4P). Neglecting the covalence, we find that κ varies between 1 (weak-field limit) and $^2/_3$ (strong-field limit).

The second term in eq 2 represents the low-symmetry (noncubic) crystal field that takes into account the distortions of the local surrounding. Combined with the spin−orbit interaction, this field gives rise to a strong magnetic anisotropy of each Co(II) and thus to the entire complex. In general, the crystal field operator can be written in the following form

$$\mathbf{H}^i_{cr} = \mathbf{L}_i\mathbf{D}_i\mathbf{L}_i \quad (4)$$

where the $\mathbf{D}_i$ tensor describes the splitting of the $^4T_{1g}$ term in the local crystal field. We suppose that for both Co ions the local axes coincide with the main axes of the $\mathbf{D}_i$ tensors and so in the local coordinate systems these tensors are

$$\mathbf{D}_i^{\mathrm{loc}} = \begin{pmatrix} -\frac{1}{3}\Delta_i + E_i & 0 & 0 \\ 0 & -\frac{1}{3}\Delta_i - E_i & 0 \\ 0 & 0 & \frac{2}{3}\Delta_i \end{pmatrix} \tag{5}$$

where Δ_i and E_i are the axial and rhombic parameters of $\mathbf{D}_i$ tensor. In the following consideration, we assume that for both Co ions these parameters are equal and thus the subscript i is omitted. To obtain the low-symmetry part of the crystal field in the molecular coordinate system, the unitary transformation should be performed.

$$\mathbf{D}_i^{\mathrm{mol}} = \mathbf{A}^{-1}(i)\mathbf{D}^{\mathrm{loc}}\mathbf{A}(i) \tag{6}$$

where the $\mathbf{A}(i)$ matrixes are given by eq 1.

The third term in the Hamiltonian (eq 2) represents the magnetic exchange between two cobalt ions. As long as the ground state of Co(II) is orbitally degenerate, the exchange interaction should contain, in general, both orbital and spin contributions. However, following the idea of Lines,[9] we assume that the exchange coupling between cobalt centers contains only an isotropic part operating with the real spins

$$\mathbf{H}_{\mathrm{ex}} = -2\mathcal{J}\mathbf{S}_1\mathbf{S}_2 \tag{7}$$

where $\mathcal{J}$ is the isotropic exchange parameter and $S_1 = S_2 = {}^3/_2$.

The last term in eq 2 is the Zeeman interaction. It consists of both spin and orbital contributions and is written as follows

$$\mathbf{H}_{\mathrm{Ze}}^i = \beta\left(g_0\mathbf{S}_i - \frac{3}{2}\kappa\mathbf{L}_i\right)\mathbf{H} \tag{8}$$

where β is the Bohr magneton and $g_0 = 2.0023$ is the electronic Landé factor. In eq 8, the spin−orbit interaction between the $^4T_{1g}$ ground state and any excited states is neglected. We show in the Appendix that after accounting for this interaction the g_0 value in eq 8 should be replaced by $g_0 + \Delta g$ where Δg depends on the Racah and cubic crystal field parameters as well as on the one-electron spin−orbit coupling constant. For the averaged values of these parameters for the high-spin Co(II) ion, Δg is about 0.12. As one can see, this value is small but not negligible. The accounting of the low-symmetry crystal field results in the anisotropy of the Δg value. However, if the distortion from the octahedral surrounding is not too strong, then this anisotropy can be neglected.

All matrix elements of the general Hamiltonian (eqs 2−8) can be calculated with the use of an irreducible tensor operator technique.[10,11] The principal values of the magnetic susceptibility are computed from the usual expression

$$\chi_u = Nk_{\mathrm{B}}T\frac{\partial^2}{\partial H_u^2}\left(\ln\sum_g \exp\left[\frac{-E_{\mathrm{g}}(H_u)}{k_{\mathrm{B}}T}\right]\right) \qquad (u = X, Y, Z) \tag{9}$$

where E_{g} represents the energy levels of the system in the external magnetic field. In eq 9, N and k_{B} are Avogadro's number and the Boltzmann constant, respectively. The powder average magnetic susceptibility is calculated as

$$\chi_{\mathrm{av}} = \frac{1}{3}(\chi_X + \chi_Y + \chi_Z) \tag{10}$$

IV. Analysis

Magnetic Data. In this section, the model described above is applied to the explanation of the magnetic behavior of the $[Co_2(\mu\text{-}OAc)_3(urea)(tmen)_2][OTf]$ complex. Detailed crystallographic data can be found elsewhere.[12,13] The Euler angles required for our calculations are $\beta_1 = 15.6°$, $\gamma_1 = -21.9°$, $\beta_2 = -15.6°$, and $\gamma_2 = 9.3°$. The magnetic properties of the investigated complex are shown in Figure 2. The best-fit parameters are listed in the Figure caption. The experimental curve is in good agreement with the calculated one. The value of the exchange parameter indicates a ferromagnetic exchange interaction between the cobalt ions.

To understand the magnetic behavior of the investigated dimer, we analyzed the low-lying energy levels of the cluster. In the first stage of this analysis, the distortion from the octahedral surroundings was neglected. Figure 3 shows the calculated energy pattern, including levels up to 400 cm^{-1}. The ferromagnetic exchange interaction between cobalt spins results in the $J = 1$ ground state. This ground state possesses an effective g factor of about 4.73. This large value of g is a result of the strong orbital contribution to the magnetic behavior of the cobalt dimer. There exists also a strong mixture of this ground state with the excited ones, possessing the same value of total angular momentum J. This mixture results in the strong temperature-independent part of the magnetic susceptibility. Expanding the energy of the ground manifold as powers of the external magnetic field H,

$$E_0 = E_0^{(0)} + E_0^{(1)}H + E_0^{(2)}H^2 + \ldots \tag{11}$$

the second-order Zeeman coefficient $E_0^{(2)} = -1.18 \times 10^{-2}$ cm^{-1} T^{-2} is obtained. The temperature-independent part of the magnetic susceptibility can be calculated by

$$\chi_{\mathrm{TIP}} = -2NE_0^{(2)} \tag{12}$$

For the investigated complex, one obtains a very large χ_{TIP} of about 2.8×10^{-2} cm^3 mol^{-1}. Because the value of the spin−orbit coupling parameter significantly exceeds the exchange coupling parameter, this TIP appears mainly because of the spin−orbit interaction.

The magnetic behavior of the cobalt dimer is explained by the interplay of two processes: the thermal population

(10) Varshalovich, D. A.; Moskalev, A. N.; Khersonskii, V. K. *Quantum Theory of Angular Momentum;* World Scientific: Singapore, 1988.
(11) Tsukerblat, B. S. *Group Theory in Chemistry and Spectroscopy;* Academic Press: London, 1994.
(12) Brown, D. A.; Errington, W.; Glass, W. K.; Haase, W.; Kemp, T. J.; Nimir, H.; Ostrovsky, S. M.; Werner, R. *Inorg. Chem.* **2001**, *40*, 5662.
(13) Werner, R. Ph.D. Thesis, Darmstadt University of Technology, 2000.

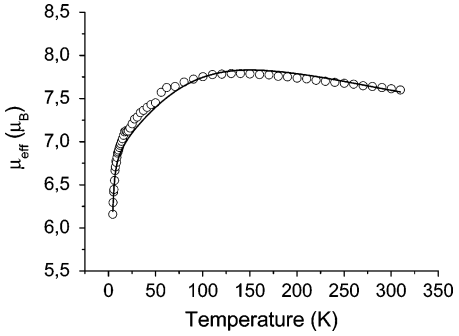

Figure 2. Effective magnetic moment for $[Co_2(\mu\text{-OAc})_3(\text{urea})(\text{tmen})_2][\text{OTf}]$. The solid line represents the best fit obtained for $\mathcal{J} = 18.0$ cm^{-1}, $\kappa = 0.7$, $\Delta = 80$ cm^{-1}, and $E = 10$ cm^{-1}.

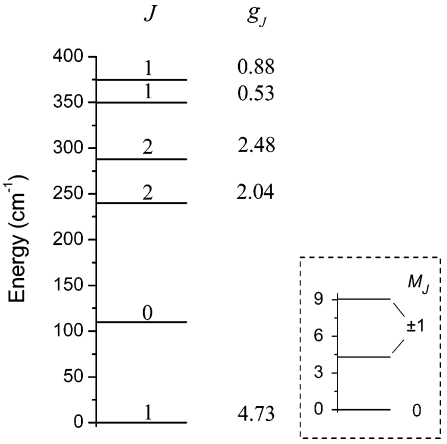

Figure 3. Energy scheme (low-lying levels) of a binuclear cobalt(II) complex for $\mathcal{J} = 18.0$ cm^{-1}, $\kappa = 0.7$, and $\Delta = 0$. In the inset, the splitting of the lowest triplet at $\Delta = 80$ cm^{-1} and $E = 10$ cm^{-1} is presented.

of the excited levels that are less magnetic than the ground one and the strong temperature-independent part of the magnetic susceptibility. With the temperature increase, the former process leads to the decrease of the effective magnetic moment whereas the latter one results in the increase of the effective magnetic moment. When the temperature is low enough and the thermal population of the excited levels is small, the latter process dominates, and the effective magnetic moment increases. At some value of temperature, the population of the levels with smaller g values becomes significant, and further temperature growth leads to the decrease of the effective magnetic moment.

The energy pattern presented in Figure 3 differs significantly from the patterns that can be obtained from the HDVV model ($J = 0, 1, 2, 3$ or $3, 2, 1, 0$ for antiferromagnetic or ferromagnetic exchange, respectively). In the framework of the present approach, we deal with four angular momenta (two spins and two orbital momenta), coupled by the exchange and SO interactions. The order of levels in Figure 3 is the result of this coupling and is determined by the interplay between the mentioned interactions.

Now we consider the effect of a small, low-symmetry crystal field. Because of the symmetry decrease, the energy levels presented in Figure 3 are split. From the magnetic point of view, the most significant factor is the behavior of the ground multiplet. The corresponding levels are presented in the inset. The ground multiplet is split into three components, with the sublevel with $M_J = 0$ being low in energy. As a result, the low-temperature value of the effective magnetic moment slightly decreases.

It should be mentioned that the values of Δ and E parameters obtained from the fitting procedure look rather small for the system with different atoms in the first coordination sphere. However, if distortion from the octahedral surroundings is strong enough, then the orbital momentum disappears and each Co(II) ion can be treated as spin $S = {}^3/_2$ with strong magnetic anisotropy. All attempts to explain the magnetic properties of the investigated compound using this spin-only model failed. Consequently, one can expect that distortion from the octahedral surroundings is small. In the next subsection, we show that the analysis of MCD data confirms the obtained values of key parameters of the system.

Magnetic Circular Dichroism Investigations. A general formula for the analysis of MCD spectra requires the calculation of the difference between molar extinction coefficients for the left and right circularly polarized light $\Delta\epsilon = \epsilon_L - \epsilon_R$. It can be written as[14]

$$\Delta\epsilon(\theta, \varphi) = -\frac{K}{Q}\sum_{i,j,k}\epsilon_{ijk}A_{zk}\sum_{g,e}\mathrm{Im}\{\langle g|m_i|e\rangle\langle e|m_j|g\rangle\}\exp\left(\frac{-E_g}{k_BT}\right) \quad (13)$$

In eq 13 g and e represent any ground and excited states, ϵ_{ijk} is the 3D antisymmetric Levi−Civita tensor, m_x, m_y, and m_z are the components of a molecule fixed transition dipole operator, $A_{zx} = \sin\theta\cos\varphi$, $A_{zy} = \sin\theta\sin\varphi$, $A_{zz} = \cos\theta$ (θ and φ describe the orientation of the magnetic field with respect to the molecule-fixed coordinate system), K is a constant that depends on the substance under examination, and Q is a partition function.

In the complex under investigation, the $J = 1$ ground state is well separated from the excited ones (Figure 3). At low enough temperatures, only these three levels are thermally accessible, and the contribution of other levels to the MCD signal can be neglected. Each of these three low-lying levels can be written as

$$|g\rangle = \sum_{M_J} C_{M_J}|J = 1, M_J\rangle \equiv \sum_M C_M|M\rangle \quad (14)$$

where the C_M coefficients ($M = 0, \pm 1$) depend on θ, φ, and the value of the external magnetic field H. Substituting eq 14 into eq 13, one obtains

(14) Oganesyan, V. S.; George, S. J.; Cheesman, M. R.; Thomson, A. J. *J. Chem. Phys.* **1999**, *110*, 762.
(15) Sugano, S.; Tanabe, Y.; Kamimura, H. *Multiplets of Transition* Ions *in Crystals;* Academic Press: New York, 1970.
(16) Abragam A.; Bleaney, B. *Electron Paramagnetic Resonance of Transitions Ions;* Clarendon Press: Oxford, U.K., 1970.
(17) Boca, R. *Theoretical Foundations of Molecular Magnetism;* Elsevier: Amsterdam, The Netherlands, 1999.

$$\Delta\epsilon(\theta, \varphi) = -\frac{K}{Q}\sum_{i,j,k}\epsilon_{ijk}A_{zk}\sum_{g,e}\sum_{M,M'} \times \mathrm{Im}\{C_M^* C_{M'}\langle M|m_i|e\rangle\langle e|m_j|M'\rangle\}\exp(-E_g/k_BT) \quad (15)$$

The experimental MCD spectrum of the investigated dimeric complex is shown in Figure 4 and is dominated by temperature-dependent contributions. The energy of the intense MCD signal is characteristic for d−d transitions. The small value of the low-symmetry crystal field obtained in the fitting procedure of the magnetic data indicates that each Co ion is in a highly symmetric environment. The ground state is orbitally degenerate, and hence the optical transitions of all polarizations should contribute to the MCD signal.

Let us regard the following combination of matrix elements

$$M_{ij}(M, M') = \sum_{i,j,k}\epsilon_{ijk}\langle M|m_i|e\rangle\langle e|m_j|M'\rangle \quad (16)$$

where $i, j = x, y, z$ and e is any excited state. Using the Wigner−Eckart theorem and the symmetry properties of Clebsch−Gordan coefficients one can obtain

$$M_{xy}(0, 0) = 0$$

$$M_{xy}(1, 1) = -M_{xy}(-1, -1) = \sqrt{2}M_{yz}(0, 1) = \sqrt{2}M_{yz}(1, 0) = \sqrt{2}M_{yz}(0, -1) = \sqrt{2}\,M_{yz}(-1, 0)$$

$$= -i\sqrt{2}M_{zx}(0, 1) = i\sqrt{2}M_{zx}(1, 0) = i\sqrt{2}M_{zx}(0, -1) = -i\sqrt{2}\,M_{zx}(-1, 0) \quad (17)$$

The preceding equation (eq 17) holds for any excited state. The same relationship applies to matrix elements $\langle M|J_k|M'\rangle$, where J_k is the kth component of the total angular momentum operator that operates within the $J = 1$ ground state. Therefore, one can write

$$M_{ij}(M, M') = R(e)\langle M|J_k|M'\rangle \quad (18)$$

where $R(e)$ represents a combination of the reduced matrix elements and depends on the excited state contributing to the MCD signal at a given wavelength. Finally, $\Delta\epsilon$ can be written as

$$\Delta\epsilon(\theta, \varphi) = -\frac{K}{Q}\sum_{e}\mathrm{Im}\{R(e)\}\sum_{k}A_{zk}\langle J_k\rangle_T \quad (19)$$

where

$$\langle J_k\rangle_T = \sum_g\langle g|J_k|g\rangle\exp(-E_g/k_BT) \quad (20)$$

Equations 19 and 20 allow us to calculate the MCD signal of the investigated dimer at any orientation of the external magnetic field with respect to the molecular coordinate system. To obtain the signal from the randomly oriented molecules in frozen Nujol, eq 19 is integrated over all magnetic field orientations

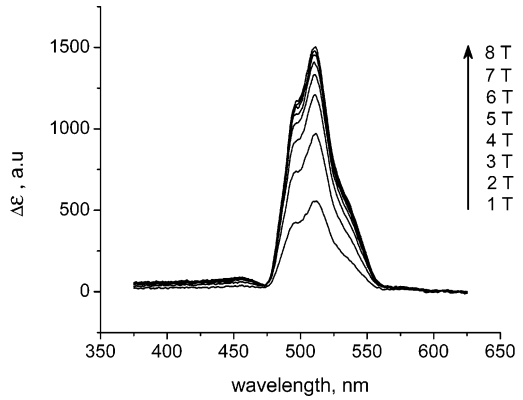

Figure 4. Experimental MCD spectrum of the $[Co_2(\mu\text{-}OAc)_3(urea)(tmen)_2]$-[OTf] complex recorded at 3.3 K.

$$\langle\Delta\epsilon\rangle = \frac{1}{4\pi}\int_0^{\pi}\int_0^{2\pi}\Delta\epsilon(\theta, \varphi)\sin\theta\,d\theta\,d\varphi \quad (21)$$

An examination of eqs 19−21 immediately leads to the following conclusion: the MCD saturation curves constructed for data collected at different wavelengths should demonstrate similar behavior. However, the magnitude of the signal is different because of the contribution of different excited states and that results in the different values of the R(e) parameter.

The experimental MCD spectrum consists of two intense bands at 495 and 510 nm. To construct the saturation magnetization curves, we recorded signal intensity at maxima of both bands. As was expected from an analysis of eqs 19−21, the intensity behavior at both wavelengths is similar (Figure 5), and after normalization curves at both wavelengths coincide. As was shown,[14] in the case of the orbitally nondegenerate ground state, the MCD signal appears because of the second-order spin−orbit mixing with nearby transitions. The forms of the magnetization curves strongly depend on the polarizations of these transitions. As a result, different curves should demonstrate different behavior. Therefore, the identical behavior of the signals recorded at various wavelengths is clear evidence of a strong orbital contribution to the MCD behavior of the investigated complex.

To determine if the MCD behavior of the investigated complex is described by the values of the key parameters obtained from the fit of magnetic data, we constructed the MCD saturation curves using the following algorithm: (i) $|M\rangle$ components of the $J = 1$ ground triplet are obtained at $\mathscr{J} = 18.0\ \mathrm{cm}^{-1}$, $\kappa = 0.7$, $\Delta = 80\ \mathrm{cm}^{-1}$, and $E = 10\ \mathrm{cm}^{-1}$; (ii) C_M coefficients are calculated as functions of H, θ, and φ by means of the diagonalization of the total (144 × 144) matrix; and (iii) MCD saturation curves are constructed using eqs 19−21. The corresponding saturation curves are presented in Figure 6. There is reasonable agreement between the experimental data and theoretical curves. This agreement confirms the applicability of the presented model to the theoretical explanation of the magneto-optical behavior of the investigated cobalt dimer. Small differences between theory and experiment can be caused by the fact that strong enough magnetic fields result in some admixture of the low-lying excited states to the $J = 1$ ground state, whereas in

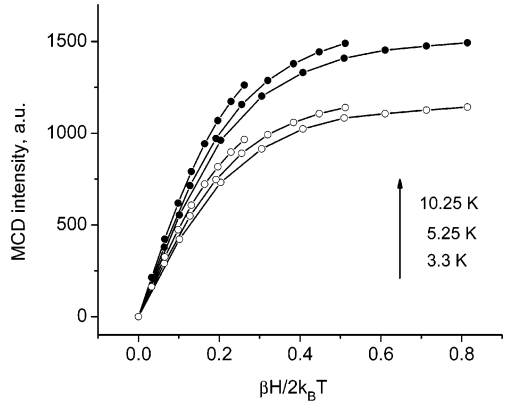

Figure 5. Experimental MCD saturation curves recorded at (●) 510 and (○) 495 nm.

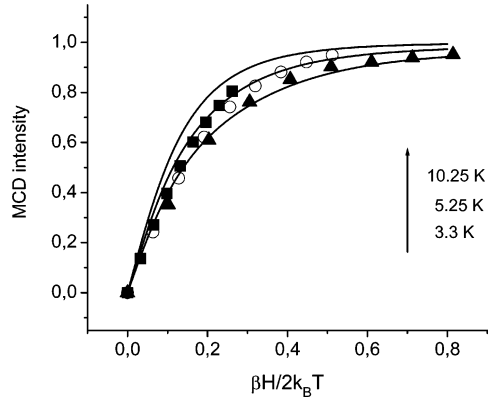

Figure 6. Comparison of calculated and measured magnetization curves. Experimental data were collected at (▲) 3.3, (○) 5.25, and (■) 10.25 K.

the present approach the contribution of these states to the MCD spectrum is neglected.

V. Conclusions

In this Article, we have reported the magnetic and MCD investigations of the $[Co_2(\mu\text{-}OAc)_3(urea)(tmen)_2][OTf]$ complex. The presence of ions with first-order orbital angular momenta results in interesting peculiarities of magnetic and MCD behavior. The model for the explanation of these peculiarities includes the isotropic exchange interaction between the real spins and spin−orbit coupling acting within the $^4T_{1g}$ ground manifold. The spin−orbit coupling with the excited terms was taken into consideration as an effective g value. By this method, the ferromagnetic exchange interaction between Co(II) ions was found. MCD studies confirm the obtained values of the key parameters. The crucial role of the orbital angular momentum in the behavior of the investigated compound was revealed.

Acknowledgment. W.H. is grateful for the financial support of the Deutsche Forschungsgemeinschaft (project Ha 782/65). We are pleased to acknowledge the support of the EUCOST program (project D21/001/00).

Appendix

The lowest orbital states of the free Co(II) ion ($3d^7$) are ^4F and ^4P. In the presence of the cubic crystal field, the ^4F state splits into the orbital triplets $^4T_{2g}$ and $^4T_{1g}$ and singlet $^4A_{2g}$, with $^4T_{1g}$ being the ground state. The ^4P term is not split and remains an orbital triplet with symmetry $^4T_{1g}$. The corresponding electron configurations are

$$\begin{aligned}
|^4T_{1g}(1)\rangle &\equiv |t_2^5(^2T_{2g})\, e^2(^3A_{2g})\, ^4T_{1g}\rangle \\
|^4T_{1g}(2)\rangle &\equiv |t_2^4(^3T_{1g})\, e^3(^2E_g)\, ^4T_{1g}\rangle \\
|^4T_{2g}\rangle &\equiv |t_2^4(^3T_{1g})\, e^3(^2E_g)\, ^4T_{2g}\rangle \\
|^4A_{2g}\rangle &\equiv |t_2^3(^4A_{2g})\, e^4(^1A_{1g})\, ^4A_{2g}\rangle
\end{aligned} \tag{A1}$$

The orbital triplets of $^4T_{1g}$ symmetry are mixed by Coulomb interaction. The energy matrix in the presence of both ligand−field and Coulomb interaction is

$$\begin{array}{c} |^4T_{1g}(1)\rangle \quad |^4T_{1g}(2)\rangle \\ \begin{pmatrix} -12B - 8Dq & 6B \\ 6B & -3B + 2Dq \end{pmatrix} \end{array} \tag{A2}$$

where B is the Racah parameter and Dq is the cubic ligand field parameter. The ground state represents a superposition of both $^4T_{1g}$ configurations

$$\Phi_{gr}(^4T_{1g}\tilde{\gamma}M) = C_1|^4T_{1g}(1)\tilde{\gamma}M\rangle + C_2|^4T_{1g}(2)\tilde{\gamma}M\rangle \tag{A3}$$

In eq A3, M is the magnetic quantum number, and $\tilde{\gamma}$ is a component of the irreducible representation T_{1g}. Coefficients C_1 and C_2 are as follows:

$$\begin{aligned}
C_1 &= \left[\frac{1}{2}\left(1 + \frac{4.5B + 5Dq}{[36B^2 + (4.5B + 5Dq)^2]^{1/2}}\right)\right]^{1/2} \\
C_2 &= \left[\frac{1}{2}\left(1 - \frac{4.5B + 5Dq}{[36B^2 + (4.5B + 5Dq)^2]^{1/2}}\right)\right]^{1/2}
\end{aligned} \tag{A4}$$

The energy of this ground-state configuration is

$$E_{gr}(^4T_{1g}) = -7.5B - 3Dq - [36B^2 + (4.5B + 5Dq)^2]^{1/2} \tag{A5}$$

Energies of the excited terms with the symmetries $^4T_{2g}$ and $^4A_{2g}$ are as follows:[15]

$$\begin{aligned}
E(^4T_{2g}) &= -15B + 2Dq \\
E(^4A_{2g}) &= -15B + 12Dq
\end{aligned} \tag{A6}$$

Let us regard the effect of spin−orbit interaction on the terms mentioned above. It can be done in two steps: (i) the interaction within each term and (ii) the coupling between components of different terms. Spin−orbit coupling splits the ground $^4T_{1g}$ term (eq A3) in a perfect octahedral ligand field into the doublet

$$\Psi_{\pm 1} = \frac{1}{\sqrt{6}}\left(-\sqrt{3}\left|a_{\mp} \pm \frac{3}{2}\right\rangle + \sqrt{2}\left|a_0 \pm \frac{1}{2}\right\rangle - \left|a_{\pm} \mp \frac{1}{2}\right\rangle\right) \tag{A7.1}$$

quartet

$$\Psi_{\pm 2} = \frac{1}{\sqrt{15}}\left(\sqrt{6}\left|a_{\mp} \pm \frac{3}{2}\right\rangle + \left|a_0 \pm \frac{1}{2}\right\rangle - 2\sqrt{2}\left|a_{\pm} \mp \frac{1}{2}\right\rangle\right)$$

$$\Psi_{\pm 3} = \frac{1}{\sqrt{5}}\left(-\sqrt{3}\left|a_0 \pm \frac{3}{2}\right\rangle + \sqrt{2}\left|a_{\pm} \pm \frac{1}{2}\right\rangle\right) \quad \text{(A7.2)}$$

and sextet states

$$\Psi_{\pm 4} = \frac{1}{\sqrt{10}}\left(\left|a_{\mp} \pm \frac{3}{2}\right\rangle + \sqrt{6}\left|a_0 \pm \frac{1}{2}\right\rangle + \sqrt{3}\left|a_{\pm} \mp \frac{1}{2}\right\rangle\right)$$

$$\Psi_{\pm 5} = \frac{1}{\sqrt{5}}\left(\sqrt{2}\left|a_0 \pm \frac{3}{2}\right\rangle + \sqrt{3}\left|a_{\pm} \pm \frac{1}{2}\right\rangle\right)$$

$$\Psi_{\pm 6} = \left|a_{\pm} \pm \frac{3}{2}\right\rangle \quad \text{(A7.3)}$$

In eqs A7.1−A7.3, $a_{\pm,0}$ are the components of the $^4T_{1g}$ term in the trigonal basis.

The $^4T_{2g}$ term is also split into three groups of levels $\Phi_{\pm 1}$, $\Phi_{\pm 2,\pm 3}$, and $\Phi_{\pm 4,\pm 5,\pm 6}$. The corresponding wave functions can be obtained from eqs A7.1−A7.3 by the following substitutions: $a_{\pm} \rightarrow x_{\pm}$ and $a_0 \rightarrow x_0$. The $^4A_{2g}$ term is not split.

The next step is to introduce into consideration the spin−orbit interaction between the ground $^4T_{1g}$ term and excited ones. It can be done using perturbation theory. There is no spin−orbit coupling between the $^4A_{2g}$ term and the ground one, so to first order, the $^4A_{2g}$ state has no effect on the magnetic properties and can be excluded from consideration. On the contrary, coupling between $^4T_{2g}$ and both $^4T_{1g}$ terms exists. To first order, one obtains

$$\Psi_i' = \Psi_i + \sum_j \frac{\langle \Phi_j | H_{SO} | \Psi_i \rangle}{E(\Psi_i) - E(\Phi_j)} \Phi_j \quad \text{(A8)}$$

Because the value of spin−orbit coupling for the high-spin Co is at least 10 times smaller than the energy gap between the $^4T_{2g}$ and $^4T_{1g}$ terms, the denominators in eq A8 can be substituted with

$$\Delta E = E(^4T_{2g}) - E_{gr}(^4T_{1g}) \quad \text{(A9)}$$

without a significant loss of accuracy.

Now let us regard the matrix elements of the Zeeman interaction within the eq A8 basis. In general, the Zeeman interaction is as follows:

$$\mathbf{H}_Z = \beta \sum_i (\mathbf{l}_i + g_0 \mathbf{s}_i)\mathbf{H} \quad \text{(A10)}$$

In eq A10, the orbital reduction due to the covalence of the cobalt−ligand bonds is neglected, and $l = 2$ is the angular orbital momentum for the d electrons. Matrix elements of operator eq A10 in the eq A8 basis can be easily calculated using the Wigner−Eckart theorem. They consist of two parts: the matrix elements of the Zeeman interaction within the $^4T_{1g}$ ground manifold and the part due to the mixture between the $^4T_{2g}$ and $^4T_{1g}$ terms. The former part can be calculated for the fictitious angular momentum $L = 1$ using the Hamiltonian of eq 8. The latter terms can be calculated for every group of levels (doublet, quartet or sextet) separately. For example, for doublet states, these additional terms to the Zeeman interaction are

$$\langle \Psi'_{\pm 1} | \mathbf{H}_Z | \Psi'_{\pm 1} \rangle^{(1)} = \frac{\beta\zeta}{\Delta E}(C_1^2 + 0.25C_2^2 - C_1C_2) \quad \text{(A11)}$$

where ζ is a one-electron spin−orbit coupling parameter, the C_i coefficients are determined in eq A4, and ΔE is given by eq A9. As one can see, the same result can be obtained by using eq A7.1 wave functions and the Hamiltonian of eq 8 with g_0 replaced by $g_0 + \Delta g$:

$$\Delta g = \frac{6\zeta}{5\Delta E}(C_1^2 + 0.25C_2^2 - C_1C_2) \quad \text{(A12)}$$

The average experimental values of the B, Dq, and ζ parameters for the Co(II) ion are taken from refs 15−17. Substitution of $B = 971$ cm^{-1}, $Dq = 840$ cm^{-1}, and $\zeta = 540$ cm^{-1} in eq A12 results in $\Delta g = 0.12$.

By repeating all considerations, we can obtain the Δg values for the quartet and sextet. It should be mentioned that there is a difference between the Δg values for different groups of levels, but this difference is small and can be ignored because the quartet and the sextet are high in energy. Therefore, the Zeeman interaction for the Co(II) ion can be presented by eq 8 with an average g value of about 2.12.

IC0514748